A Hydrothermal Seedling Emergence Model for Giant Ragweed (*Ambrosia trifida*)

Brian J. Schutte, Emilie E. Regnier, S. Kent Harrison, Jerron T. Schmoll, Kurt Spokas, and Frank Forcella*

Late-season giant ragweed emergence in Ohio crop fields complicates decisions concerning the optimum time to implement control measures. Our objectives were to develop a hydrothermal time emergence model for a late-emerging biotype and validate the model in a variety of locations and burial environments. To develop the model, giant ragweed seedlings were counted and removed weekly each growing season from 2000 to 2003 in a fallow field located in west central Ohio. Weather data, soil characteristics and geographic location were used to predict soil thermal and moisture conditions with the Soil Temperature and Moisture Model (STM^2). Hydrothermal time (θ_{HT}) initiated March 1 and base values were extrapolated from the literature (T_b = 2 C, ψ_b = −10 MPa). Cumulative percent emergence initially increased rapidly and reached 60% of maximum by late April (approximately 400 θ_{HT}), leveled off for a period in May, and increased again at a lower rate before concluding in late July (approximately 2,300 θ_{HT}). The period in May when few seedlings emerged was not subject to soil temperatures or water potentials less than the θ_{HT} base values. The biphasic pattern of emergence was modeled with two successive Weibull models that were validated in 2005 in a tilled and a no-tillage environment and in 2006 at a separate location in a no-tillage environment. Root-mean-square values for comparing actual and model predicted cumulative emergence values ranged from 8.0 to 9.5%, indicating a high degree of accuracy. This experiment demonstrated an approach to emergence modeling that can be used to forecast emergence on a local basis according to weed biotype and easily obtainable soil and weather data.

Nomenclature: Giant ragweed, *Ambrosia trifida* L.

Key words: Weed ecology, weed management decision tool, soil moisture, soil temperature.

Models that estimate the timing of weed seedling emergence are valuable management decision tools that can be used to optimize weed control schedules (Forcella 1998). Typically, seedling emergence models are developed by making species-level assumptions about seed germination (Benech-Arnold and Sánchez 1995; Forcella et al. 2000; Grundy 2003), but, for many species, germination requirements vary among populations. For example, little mallow (*Malva parviflora* L.) seeds from wetter regions of the Australian wheat belt are highly dormant and require many cycles of fluctuating temperatures for germination, whereas little mallow seeds from drier regions of the Australian wheat belt exhibit low levels of dormancy and require few cycles of alternating temperatures for germination (Michael et al. 2006). Tall waterhemp [*Amaranthus tuberculatus* (Moq.) Sauer] seeds from the western U.S. corn belt are highly dormant and have prolonged stratification requirements for germination, whereas common waterhemp seeds from the eastern U.S. corn belt show reduced seed dormancy and relatively short stratification requirements for germination (Leon et al. 2006). Inherent differences in seed germination among weed populations limit wide-scale applicability of emergence forecasting tools.

The geographic limitations of emergence models were demonstrated by Grundy et al. (2003), who tested a generic model to predict emergence timing of common chickweed [*Stellaria media* (L.) Vill.] seeds collected from across Europe. Although they found general agreement between predicted and observed common chickweed emergence, model accuracy

varied among populations. Here we improve emergence predictions for local giant ragweed populations by accounting for the inherent differences in seedling emergence periodicity that occur among locations.

Giant ragweed is one of the most competitive and troublesome weeds in the eastern U.S. corn belt (Gibson et al. 2005; Harrison et al. 2001; Webster et al. 1994). In Ohio crop fields, management of giant ragweed is difficult because of a prolonged period of seedling emergence (Sprague et al. 2004), which allows giant ragweed to escape control measures and compete with the crop. Harrison et al. (2001) determined that giant ragweed seedlings that emerged 4 wk after corn (*Zea mays* L.) emergence reduced yield at a rate of 1% per weed per 10 m^2 and added to the weed seedbank. Therefore, effective giant ragweed management requires accurate predictions of late-season seedling emergence.

Giant ragweed emergence periodicity is predicted by WeedCast, a computer software program that provides hydrothermal time emergence models for many weed species common to the U.S. corn belt (Forcella 1998). Hydrothermal time (θ_{HT}) is a growing degree day (GDD) measurement that accumulates when daily average soil water potentials and temperatures are greater than threshold values below which seedling emergence cannot occur (Gummerson 1986). Users of WeedCast provide their local soil conditions and local weather data and the software gives predictions of seedling emergence based on emergence characteristics of weed populations sampled across the U.S. corn belt. The populations that were studied during the development of WeedCast were assumed to represent populations throughout the region (Forcella 1998).

Giant ragweed seed germination requirements and seedling emergence patterns differ among populations (Schutte et al. 2006a). Sprague et al. (2004) collected giant ragweed ''involucral achenes'' (hereafter called seeds) from across the U.S. corn belt and buried them in a common garden. Seeds that originated from the western U.S. corn belt (Iowa) produced seedlings in a rapid flush during early April, whereas

*First, second, third, and fourth authors: Department of Horticulture and Crop Science, The Ohio State University, 2021 Coffey Road, Columbus, OH 43210. Fifth and sixth authors: United States Department of Agriculture—Agricultural Research Service North Central Soil Conservation Research Laboratory, 803 Iowa Avenue, Morris, MN 56267. Current address of first author: United States Department of Agriculture—Agricultural Research Service, Invasive Weed Management Unit, 1102 South Goodwin Avenue, Urbana, IL 61801. Corresponding author's E-mail: brian.schutte@ars.usda.gov

seeds that originated from the eastern U.S. corn belt (Illinois and Ohio) produced seedlings in a more gradual flush that extended into late July. The inherent differences in emergence periodicity among giant ragweed populations confound emergence predictions for the broad U.S. corn belt. Specifically, the prolonged emergence period of giant ragweed in Ohio is not described by hydrothermal time models in WeedCast (Schutte, unpublished data).

The objectives of this research were (1) to develop a hydrothermal time seedling emergence model for a giant ragweed biotype with a prolonged period of seedling emergence, and (2) to validate the model in a variety of locations and burial environments.

Materials and Methods

Seedling Emergence Model Development. We used observations of giant ragweed seedling emergence and simulated soil environments based on meteorological records, soil characteristics and geographic locations to develop a giant ragweed emergence model. An experiment was conducted during 2001, 2002, and 2003 at the Western Branch Experiment Station of the Ohio Agricultural Research and Development Center near South Charleston, OH (39°52′N, 83°40′W; elevation 340 m). The study site was a no-tillage fallow field divided into four replicates. The site had a 19-yr history of giant ragweed infestation in a corn–soybean [*Glycine max* (L.) Merr.] rotation. The soil was a Crosby silt loam (fine, mixed, active, mesic Aeric Epiaqualf) with 15% sand, 65% silt, 20% clay, and 2.2% organic matter in the Ap horizon.

Quadrats were established at the beginning of each year and were maintained free of vegetation by hand weeding. Beginning March 1 and continuing to September 1, giant ragweed seedlings in two 1-m^2 quadrats per replicate were counted and removed at weekly intervals. Seedling emergence was defined as full expansion of cotyledons, and seedlings were pulled from soil with minimal soil disturbance. Also at weekly intervals, depth of emergence was determined for 10 seedlings per replicate. Seedling emergence depth was measured by marking the soil boundary on the seedling hypocotyl prior to removal, and then measuring the hypocotyl length from the soil boundary to the root hair tuft after removal. At the end of the year, weekly emergence observations for each replicate were converted to cumulative percent emergence. Mean cumulative emergence of 100% indicated the day of final emergence.

Soil microclimate at the 1-cm depth was simulated by the Soil Temperature and Moisture Model (STM^2) (Spokas et al. 2007). STM^2 establishes a one-dimensional vertical profile from the soil surface down to 1.8 m, sectioned into discrete nodes to define soil microclimates at specific depths. Fluxes in and out of the system are primarily governed by atmospheric conditions at the soil surface. STM^2 simulates incident solar radiation with SolarCalc, a model that estimates hourly solar radiation based on latitude, longitude, and elevation of the field site, along with daily precipitation, and daily minimum and maximum air temperatures (Spokas and Forcella 2006). To estimate soil water potential, STM^2 requires data on soil texture, soil organic matter, and initial soil moisture. We assumed soil was saturated at the beginning of the experiment. A summary of the total inputs for STM^2 include latitude, longitude, elevation, daily precipita-

tion, daily minimum and maximum temperature, soil texture, and soil organic matter. Meteorological data for STM^2 were approximately 0.5 km from the study site and collected by a weather station programmed to record atmospheric conditions at 2 m every 5 min. In addition, temperature probes linked to data loggers[1] monitored soil temperatures at the 1-cm depth within the research plots at 5-min intervals.

Simulated soil temperatures and water potentials were used to calculate hydrothermal time (θ_{HT}) with the use of Equation 1

$$\theta_{HT} = \theta_H \cdot \theta_T \qquad [1]$$

where $\theta_H = 1$ when $\psi > \psi_b$, otherwise $\theta_H = 0$; and $\theta_T = T - T_b$ when $T > T_b$, otherwise $\theta_T = 0$. Daily average soil water potential at 1 cm is represented by ψ, ψ_b is base water potential for seedling emergence, T is daily average soil temperature at 1 cm, and T_b is base temperature for seedling emergence (Roman et al. 2000); 2 C for giant ragweed (Abul-Fatih and Bazzaz 1979). To estimate the base water potential of giant ragweed emergence, we utilized the findings of Abul-Fatih and Bazzaz (1979) in which giant ragweed seed germination was measured along a gradient of soil water content. We converted soil water content to soil water potential from curves characteristic for the soil textures reported in their study (Campbell 1977). Hydrothermal time accumulated from March 1. Typically, giant ragweed emergence begins mid- to late March in Ohio.

Mean cumulative percent emergence for each year was plotted as a function of day of year with hydrothermal time superimposed on the x-axis. To predict the pattern of seedling emergence, cumulative percent emergence values were compared to hydrothermal time with the Weibull function (Equation 2)

$$Y = M\{1 - \exp[-k(\theta_{HT} - z)^c]\}, \qquad [2]$$

where Y is the cumulative percent emergence, M is the asymptote, k is the rate of increase, θ_{HT} is hydrothermal time, z is θ_{HT} of first emergence, and c is a curve shape parameter (Brown and Mayer 1988). The Weibull function was fit to observed emergence values through an iterative process in which the following parameters were manually adjusted: asymptote (M), rate (k) lag phase (z), and curve shape (c), as well as the base water potential for seedling emergence (ψ_b). The model parameters (k and c) were further adjusted by a nonlinear regression procedure in SAS^2 (PROC NLIN) that used the Gauss–Newton algorithm. Agreement between predicted and actual emergence values was determined with the root-mean-square error (RMSE) (Equation 3)

$$\text{RMSE} = \sqrt{1/n \sum_{i=1}^{n} (x_1 - y_1)^2} \qquad [3]$$

where x_i represents actual cumulative percent seedling emergence, y_i is predicted cumulative percent seedling emergence, and n is the number of observations (Mayer and Butler 1993). RMSE provided a measurement of the typical difference between predicted and actual values in units of percent seedling emergence. The lowest RMSE value indicated that emergence model fit had been optimized. The end result was a single model that described seedling emergence for 2001, 2002, and 2003.

Emergence Model Validation. The seedling emergence model was validated at South Charleston, OH in 2005 and
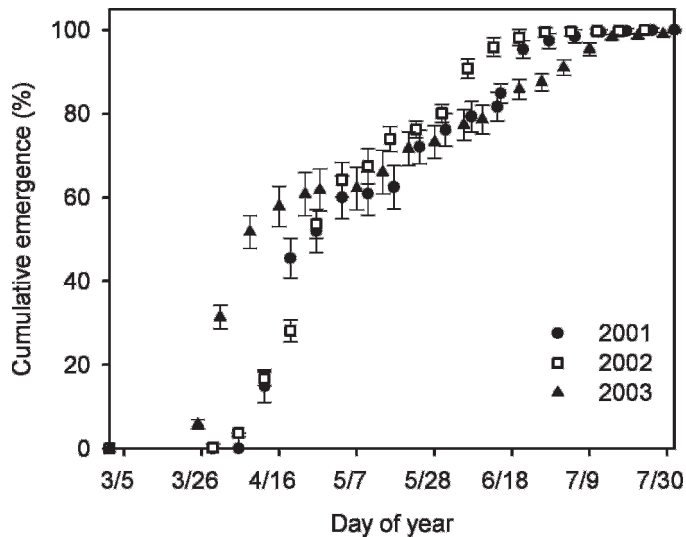
Figure 1. Giant ragweed seedling emergence in a no-tillage, fallow field in South Charleston, OH. The study site had a 19-yr history of giant ragweed infestation in a corn–soybean rotation. Seedling emergence was determined at weekly intervals from March 1 to September 1 during 2001, 2002, and 2003, but seedlings were not found after July 30. Symbols represent observed emergence and are the means of four replicates with standard errors.

at Columbus, OH in 2006. The South Charleston site included tilled and no-tillage fields. The tilled field was chisel-plowed in the fall prior to planting and received two passes with a disk-harrow cultivator during the spring. The Columbus site was a no-tillage field at The Ohio State University Waterman Agricultural and Natural Resources Laboratory (39°59′N, 83°01′W; elevation 240 km). Soil at the Columbus site was a Kokomo silty clay loam (fine, mixed, mesic Typic Argiaquolls) with 18% sand, 41% silt, 41% clay, and 2.8% organic matter in the Ap horizon. At each site, precipitation and air temperature at 2 m were recorded at 5-m intervals by an on-site weather station. Validation environments were divided into four blocks. Within each block, giant ragweed seedlings were counted and removed from two permanent 1-m^2 quadrats at weekly intervals that began March 1 and continued until September 1. Seedling emergence observations for each replicate were converted to cumulative percent of total emergence, averaged across replicates, and plotted as a function of hydrothermal time. Hydrothermal time was calculated with soil environment data from STM^2. Emergence pattern predictions based on hydrothermal time were superimposed on plots of actual seedling emergence. The difference between predicted and actual seedling emergence values was assessed by RMSE (Equation 3).

Results and Discussion

Seedling Emergence Model Development. When examined across years, the day of first emergence ranged from March 25 to April 5, and the day of final emergence ranged from July 24 to July 30. The general pattern of emergence was as follows: rapid increase to 60% of maximum during April, then a lag in early May, followed by an increase at a lower rate before concluding in late July (Figure 1). The lag period in May was indicated by a plateau in cumulative percent emergence and was more pronounced during 2001 and 2003 than 2002. However, emergence during all years was characterized by a
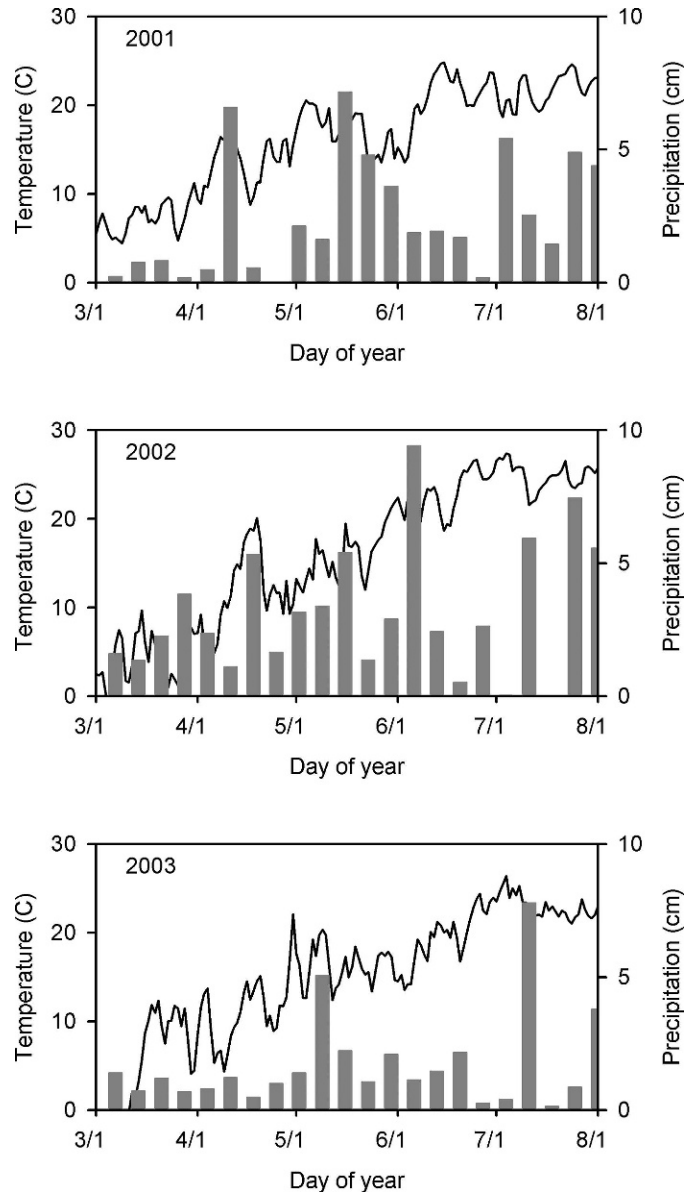

Figure 2. Daily average soil temperatures (solid line) and weekly total precipitation (shaded bars) at South Charleston, OH during the giant ragweed emergence period. Soil temperatures at the 1-cm depth were determined every 5 min at four locations within the study site. Temperature data were averaged across locations and daily average soil temperatures were calculated as [(minimum temperature + maximum temperature)/2]. Precipitation data were collected 0.5 km from the study site.

relatively quick flush followed a more gradual flush. This biphasic pattern of emergence is consistent with Ohio growers' anecdotal reports of two giant ragweed seedling emergence flushes during the growing season.

Causal factors for the biphasic pattern of emergence are not yet understood. Harrison et al. (2007) determined that rates of giant ragweed seed dormancy loss and germination timing were influenced by the depth at which seeds were buried. But, in this experiment, mean emergence depth for seedlings in the first flush (1.31 ± 0.10 cm) did not differ from mean emergence depth for seedlings in the second flush (1.27 ± 0.07 cm) (P = 0.86). Therefore, the biphasic pattern of emergence was not because of differential burial depths. Other researchers have attributed interruptions in the progress of cumulative percent emergence to suboptimal soil tempera-

Table 1. Development of a seedling emergence model in a no-tillage, fallow field in South Charleston, OH. The study site had a 19-yr history of giant ragweed infestation in a corn–soybean rotation. Emergence was determined at weekly intervals from March 1 to September 1 during 2001, 2002, and 2003. The four-parameter Weibull model was fit to cumulative percent emergence plotted as function of day of year with hydrothermal time (θ_{HT}) superimposed on the x-axis.

Emergence period[a]	Weibull model parameters[b]				θ_{HT} base values		Root-mean-square error[c] (% cumulative emergence)
	M	z	c	k	T_b (C)	ψ_b (MPa)	
Prelag phase	60	60	1.60	2.7×10^{-4}	2.0	-10	9.17
Postlag phase	40	600	1.23	6.0×10^{-4}	2.0	-30	4.95

[a] The emergence period was divided into two phases that were separated by the lag in cumulative percent emergence that occurred each year during early May.

[b] Weibull models were in the form $Y = M\{1 - \exp[-k(\theta_{HT} - z)^c]\}$, where Y is the cumulative percent emergence, M is the asymptote, k is the rate of increase, θ_{HT} is hydrothermal time accumulated from March 1, z is θ_{HT} of first emergence, and c is a curve shape parameter.

[c] Root-mean-square error provides an indication of the typical difference between predicted and actual values.

tures and moisture conditions (Benech-Arnold et al. 2000); however, the period in May when few seedlings emerged was not subject to soil temperatures less than the base temperature for seedling emergence (2 C) or precipitation deficits (Figure 2). Accordingly, hydrothermal time continued to accumulate during May, and emergence showed a temporary lag phase before resuming at a lower rate.

The biphasic pattern of emergence may have been a consequence of seed-to-seed variation in hydrothermal time requirements for seedling emergence. Typically, seed-to-seed variation in germination behavior is continuous (Bradford 1996), and, as a result, cumulative seedling emergence in response to hydrothermal time is described by a single sigmoidal curve (for example, see Shrestha et al. 1999). Two distinct emergence flushes suggest that subpopulations exist within the seed population itself. Delayed emergence can be adaptive in crop fields (Clements et al. 2004; Mortimer 1997), and thus the biphasic pattern of emergence may represent an evolutionary response to agricultural selection pressures. Along these lines, Hartnett et al. (1987) suggested that giant ragweed populations evolved during old-field succession to produce more seedlings earlier in the growing season, and Schutte et al. (2006b) determined that emergence patterns vary among giant ragweed phenotypes in agricultural fields. To clarify the evolutionary significance and the origins of the biphasic emergence pattern, subsequent research should study the heritability of seedling emergence patterns in giant ragweed.

A single, four-parameter Weibull model did not accurately describe the biphasic pattern of emergence (data not shown). Therefore, we divided the emergence period into pre- and postlag phases and modeled cumulative percent emergence with two successive Weibull functions (Table 1). Hydrothermal time was calculated with soil temperature and moisture data produced with the Soil Temperature and Moisture Model (STM^2) (Spokas et al. 2007). We believe STM^2 simulated the soil environment with a high degree of accuracy because daily average soil temperatures calculated with actual values were highly correlated with daily average soil temperatures calculated with STM^2 values ($r = 0.98$, P < 0.001).

To optimize emergence model fit, each model required a unique base water potential. The base water potential was initially extrapolated from the literature as -10 MPa and then iteratively adjusted until the difference between predicted and observed seedling emergence was minimized. The low base water potentials in our emergence models indicate that giant ragweed seedling emergence was insensitive to dry conditions in the top 1 cm of soil. Although the 1-cm depth was close to the overall mean emergence depth (1.29 $\pm$ 0.19 cm), the maximum emergence depth was 7 cm.

Therefore, soil environment predictions did not accurately reflect the microenvironment of each seed. Nonetheless, our results indicate that giant ragweed emergence occurred during periods in which the top layers of soil were relatively dry. Giant ragweed seeds can be up to 11 mm wide and 14 mm long, and are substantially larger than seeds of most annual weed species (Sako et al. 2001). Other researchers hypothesized that increased seed size enables seedling emergence under low soil moisture because larger seeds produce longer radicles that can access deeper water resources, contain relatively more nutritional reserves, and have decreased metabolic rates (reviewed by Leishman et al. 2000).

Seedling Emergence Model Validation. Two successive Weibull models predicted seedling emergence in different locations and tillage environments with reasonable accuracy (Figure 3). The RMSE values of this experiment (8.2, 8.0, and 9.5% cumulative emergence) compared favorably to other seedling emergence models. Ekeleme et al. (2005) reported a hydrothermal time seedling emergence model for tropic ageratum (*Ageratum conyzoides* L.) with RMSE values ranging from 5.8 to 10.1% cumulative emergence, and Roman et al. (2000) developed hydrothermal time seedling emergence models for common lambsquarters (*Chenopodium album* L.) with RMSE values that ranged from 6.5 to 37.1% cumulative emergence.

Prior to this experiment, the prolonged emergence period of the giant ragweed biotype in Ohio agricultural fields was not described by a model developed for the broader U.S. corn belt (Schutte, unpublished data). The applicability of our localized model outside of central Ohio is unknown, but, as demonstrated in this experiment, model calibration with local weed biotypes could be accomplished with one growing season for model development followed by a growing season for model validation. In addition to emergence pattern variation on a broad scale, emergence periodicity may differ among weed populations in nearby crop fields because agronomic practices can influence levels of seed dormancy (Clements et al. 2004). For example, frequent summer fallowing increased seed dormancy (decreased germination capacity at 20 C in darkness) of wild oat (*Avena fatua* L.) in cultivated fields in Saskatchewan (Jana and Thai 1987; Naylor and Jana 1976). Organic farming was associated with decreased seed dormancy (increased germination capacity at 30/25 C, 16/8-h photoperiods) and increased late-season emergence of Powell amaranth (*Amaranthus powellii* S. Wats.) among vegetable farms in central New York (Brainard et al. 2006). Field-to-field variation in seed dormancy and emergence periodicity suggests a need for increasingly localized weed emergence models.
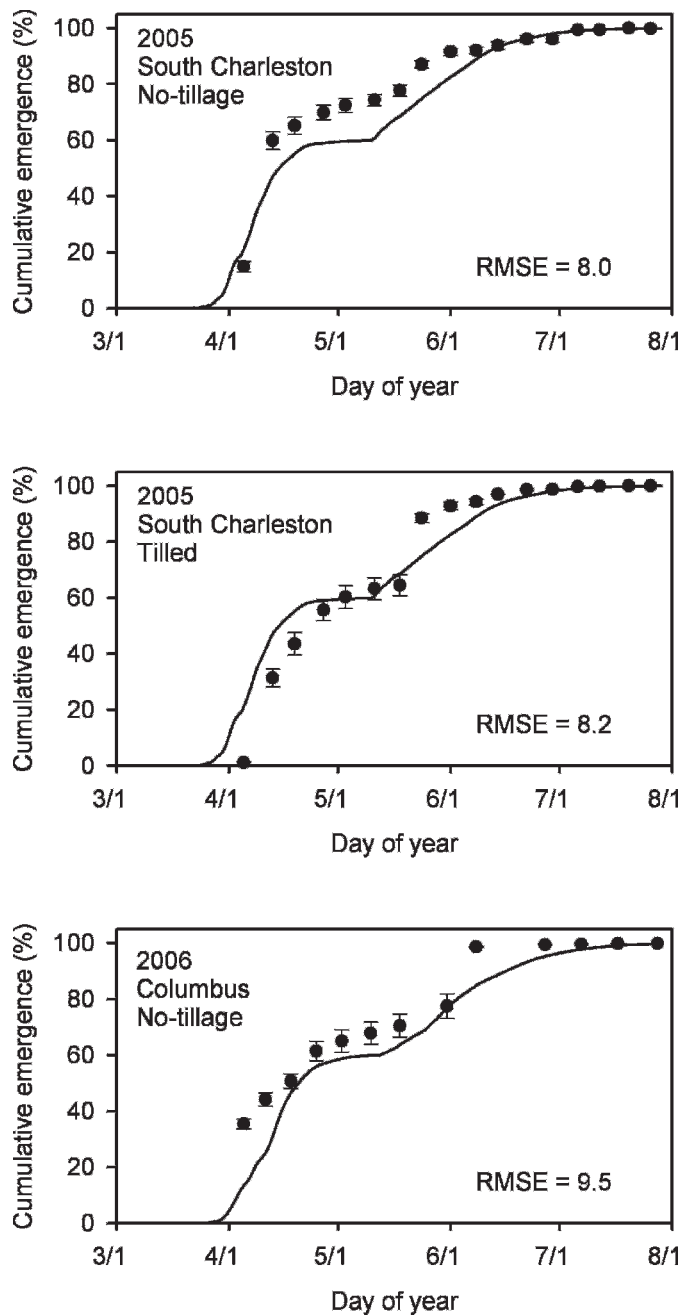
Figure 3. Hydrothermal seedling emergence model validation in fallow fields at South Charleston, OH under tilled and no-tillage conditions, and at Columbus, OH under no-tillage conditions. Solid lines represent predicted emergence with the use of model parameters presented in Table 1. Closed circles represent observed emergence and are the means of four replicates with standard errors. Root-mean-square error (RMSE) values are in units of percent cumulative emergence.

There are several approaches to emergence modeling, and differences among them include the degree of developmental complexity (Forcella et al. 2000; Grundy 2003). One modeling technique utilizes observations of emergence during past growing seasons to produce predictions based on the day of year (Egley and Williams 1991; Ogg and Dawson 1984). Day-of-year emergence models can be straightforward to develop, but their predictions can fail during years when atypical weather occurs during the normal emergence period. Another emergence modeling technique separately quantifies the components of emergence (seed dormancy loss, seed germination, and pre-emergence seedling growth) over a range of controlled conditions, then extrapolates the results to field settings (Benech-Arnold and Sánchez 1995; Vleeshouwers 1997). These reductive seedling emergence models are responsive to atypical weather, but their development requires extensive experimentation.

Hydrothermal time and thermal time emergence models that base predictions on field observations during previous growing seasons offer relatively robust predictions and simple development (Forcella et al. 2000). Compared to thermal time, hydrothermal time calculations require additional data that can be difficult to obtain (Myers et al. 2004); however, the extra information from hydrothermal time may improve seedling emergence predictions (Grundy and Mead 2000). Data acquisition for hydrothermal time calculations is eased by soil environment models, such as STM^2, that simulate the soil environment based on readily available information. Simplicity of hydrothermal emergence model development may facilitate relatively rapid development of localized emergence forecasts for species that exhibit biotype variation in seasonal emergence patterns.

Potential Application of Results. The emergence model presented in this article can be used as a management decision tool for a giant ragweed biotype with a prolonged period of seedling emergence. Long-term (i.e., several months) emergence forecasts indicate how lasting residual herbicides need to be for control of giant ragweed. Short-term (i.e. 1-wk) emergence forecasts provide information on the optimum time for postemergence herbicide applications and mechanical control procedures.

In addition to immediate implications on giant ragweed management, the model presented in this article points to future research projects that may improve giant ragweed management in the long run. We propose research on delayed planting of summer annual crops as a tactic to control giant ragweed. This proposal is based on the following assumptions: 1) late-season emergence will occur every year, and 2) seedlings that emerge after crop emergence will be competitive, reproductive, and difficult to control (Gibson et al. 2005; Harrison et al. 2001; Webster et al. 1994). Therefore, a practical solution for reducing giant ragweed populations is to minimize the percentage of seedlings that emerge after the crop. Furthermore, the emergence model technique provides a relatively efficient method to monitor giant ragweed populations for change in emergence patterns over time. This could improve our understanding of weed evolution and help identify important management factors that most strongly select for different emergence biotypes.

Finally, the emergence model presented in this article can be improved by coupling emergence predictions with data on the number of germinable seeds in the giant ragweed seedbank. Such a model would predict giant ragweed emergence periodicity and density, thus providing a more complete emergence forecast.

Sources of Materials

[1] HOBO H8® Pro Series temperature data loggers, Onset, P.O. Box 3450, Pocasset, MA 02559-3450.
[2] SAS software for Windows, Version 9.1.3, SAS Institute Inc., Cary, NC 27513.

Literature Cited

Abul-Fatih, H. A. and F. A. Bazzaz. 1979. The biology of *Ambrosia trifida* L. II. Germination, emergence, growth and survival. New Phytol. 83:817–827.

Benech-Arnold, R. L. and R. A. Sánchez. 1995. Modeling weed seed germination. Pages 545–566 *in* J. Kigel and G. Galili, eds. Seed Development and Germination. New York, NY: Marcel Dekker.

Benech-Arnold, R. L., R. A. Sanchez, F. Forcella, B. C. Kruk, and C. M. Ghersa. 2000. Environmental control of dormancy in weed seed banks in soil. Field Crops Res. 67:105–122.

Bradford, K. J. 1996. Population-based models describing seed dormancy behaviour: implications for experimental design and interpretation. Pages 313–339 *in* G. A. Lang, ed. Plant Dormancy: Physiology, Biochemistry and Molecular Biology. Wallingford, UK: CAB International.

Brainard, D. C., A. DiTommaso, and C. L. Mohler. 2006. Intraspecific variation in germination response to ammonium nitrate of Powell amaranth (*Amaranthus powellii*) seeds originating from organic vs. conventional vegetable farms. Weed Sci. 54:435–442.

Brown, R. F. and D. G. Mayer. 1988. Representing cumulative germination. 2. The use of the Weibull function and other empirically derived curves. Ann. Bot. 61:127–138.

Campbell, G. S. 1977. An Introduction to Environmental Biophysics. New York: Springer-Verlag. Pp. 1–31.

Clements, D. R., A. DiTommaso, N. Jordan, B. D. Booth, J. Cardina, D. Doohan, C. L. Mohler, S. D. Murphy, and C. J. Swanton. 2004. Adaptability of plants invading North American cropland. Agric. Ecosyst. Environ. 104:379–398.

Egley, G. H. and R. D. Williams. 1991. Emergence periodicity of six summer annual weed species. Weed Sci. 39:595–600.

Ekeleme, F., F. Forcella, D. W. Archer, I. O. Akobundu, and D. Chikoye. 2005. Seedling emergence model for tropic ageratum (*Ageratum conyzoides*). Weed Sci. 53:55–61.

Forcella, F. 1998. Real-time assessment of seed dormancy and seedling growth for weed management. Seed Sci. Res. 8:201–209.

Forcella, F., R. L. Benech-Arnold, R. A. Sanchez, and C. M. Ghersa. 2000. Modeling seedling emergence. Field Crops Res. 67:123–139.

Gibson, K. D., W. G. Johnson, and D. E. Hillger. 2005. Farmer perceptions of problematic corn and soybean weeds in Indiana. Weed Technol. 19:1065–1070.

Grundy, A. C. 2003. Predicting weed emergence: a review of approaches and future challenges. Weed Res. 43:1–11.

Grundy, A. C. and A. Mead. 2000. Modeling weed emergence as a function of meteorological records. Weed Sci. 48:594–603.

Grundy, A. C., N.C.B. Peters, I. A. Rasmussen, K. M. Hartmann, M. Sattin, L. Andersson, A. Mead, A. J. Murdoch, and F. Forcella. 2003. Emergence of *Chenopodium album* and *Stellaria media* of different origins under different climatic conditions. Weed Res. 43:163–176.

Gummerson, R. J. 1986. The effect of constant temperature and osmotic potentials on the germination of sugar beet. J. Exp. Bot. 37:729–741.

Harrison, S. K., E. E. Regnier, J. T. Schmoll, and J. M. Harrison. 2007. Seed size and burial effects on giant ragweed (*Ambrosia trifida*) emergence and seed demise. Weed Sci. 55:16–22.

Harrison, S. K., E. E. Regnier, J. T. Schmoll, and J. E. Webb. 2001. Competition and fecundity of giant ragweed in corn. Weed Sci. 49:224–229.

Hartnett, D. C., B. B. Hartnett, and F. A. Bazzaz. 1987. Persistence of *Ambrosia trifida* populations in old fields and responses to successional changes. Am. J. Bot. 74:1239–1248.

Jana, S. and K. M. Thai. 1987. Patterns of changes of dormant genotypes in *Avena fatua* populations under different agricultural conditions. Can. J. Bot. 65:1741–1745.

Leishman, M. R., I. J. Wright, A. T. Moles, and M. Westoby. 2000. The evolutionary ecology of seed size. Pages 31–58 *in* M. Fenner, ed. Seeds: The Ecology of Regeneration in Plant Communities. 2nd ed. New York, NY: CAB International.

Leon, R. G., D. C. Bassham, and M.D.K. Owen. 2006. Germination and proteome analyses reveal intraspecific variation in seed dormancy regulation in common waterhemp (*Amaranthus tuberculatus*). Weed Sci. 54:305–315.

Mayer, D. G. and D. G. Butler. 1993. Statistical validation. Ecol. Model. 68:21–32.

Michael, P. J., K. J. Steadman, and J. A. Plummer. 2006. Climatic regulation of seed dormancy and emergence of diverse *Malva parviflora* populations from a Mediterranean-type environment. Seed Sci. Res. 16:273–281.

Mortimer, A. M. 1997. Phenological adaptation in weeds—an evolutionary response to the use of herbicides? Pestic. Sci. 51:299–304.

Myers, M., W. S. Curran, M. J. VanGessel, D. D. Calvin, D. A. Mortensen, B. A. Majek, H. D. Kartsen, and G. W. Roth. 2004. Predicting weed emergence for eight annual species in the northeastern United States. Weed Sci. 52:913–919.

Naylor, J. M. and S. Jana. 1976. Genetic adaptation for seed dormancy in *Avena fatua*. Can. J. Bot. 54:306–312.

Ogg, A. G. and J. H. Dawson. 1984. Time of emergence of eight weed species. Weed Sci. 32:327–335.

Roman, E. S., S. D. Murphy, and C. J. Swanton. 2000. Simulation of *Chenopodium album* seedling emergence. Weed Sci. 48:217–224.

Sako, Y., E. E. Regnier, T. Daoust, K. Fujimura, S. K. Harrison, and M. B. McDonald. 2001. Computer image analysis and classification of giant ragweed seeds. Weed Sci. 49:738–745.

Schutte, B. J., E. E. Regnier, and S. K. Harrison. 2006a. Dissection of divergent emergence patterns in agricultural and successional giant ragweed populations. Proc. Weed Sci. Soc. Am. 46:49.

Schutte, B. J., E. E. Regnier, and S. K. Harrison. 2006b. Maternal plant as sources of emergence variation within giant ragweed (*Ambrosia trifida* L.) populations. Abstr. Weed. Sci. Soc. Am. 46:29.

Shrestha, A., E. S. Roman, A. G. Thomas, and C. J. Swanton. 1999. Modeling germination and shoot-radicle elongation of *Ambrosia artemisiifolia*. Weed Sci. 47:557–562.

Spokas, K. and F. Forcella. 2006. Estimating hourly incoming solar radiation from limited meteorological data. Weed Sci. 54:182–189.

Spokas, K., F. Forcella, D. Archer, D. Peterson, and S. Miller. 2007. Improving weed germination models by incorporating seed microclimate and translocation by tillage. Proc. Weed Sci. Soc. Am. 44:60.

Sprague, C. L., L. M. Wax, R. G. Hartzler, and S. K. Harrison. 2004. Variations in emergence patterns of giant ragweed biotypes from Ohio, Illinois, and Iowa. Abstr. Weed Sci. Soc. Am. 44:60.

Vleeshouwers, L. M. 1997. Modelling the effect of temperature, soil penetration resistance, burial depth and seed weight on pre-emergence growth of weeds. Ann. Bot. 79:553–563.

Webster, T. M., M. M. Loux, E. E. Regnier, and S. K. Harrison. 1994. Giant ragweed (*Ambrosia trifida*) canopy architecture and interference studies in soybean (*Glycine max*). Weed Technol. 8:559–564.